

Measurement of Dijet Angular Distributions at $\sqrt{s} = 1.96$ TeV and Searches for Quark Compositeness and Extra Spatial Dimensions

V.M. Abazov³⁷, B. Abbott⁷⁵, M. Abolins⁶⁵, B.S. Acharya³⁰, M. Adams⁵¹, T. Adams⁴⁹, E. Aguilo⁶, M. Ahsan⁵⁹, G.D. Alexeev³⁷, G. Alkhalaf⁴¹, A. Alton^{64,a}, G. Alverson⁶³, G.A. Alves², L.S. Ancu³⁶, T. Andeen⁵³, M.S. Anzelc⁵³, M. Aoki⁵⁰, Y. Arnoud¹⁴, M. Arov⁶⁰, M. Arthaud¹⁸, A. Askew^{49,b}, B. Åsman⁴², O. Atramentov^{49,b}, C. Avila⁸, J. BackusMayes⁸², F. Badaud¹³, L. Bagby⁵⁰, B. Baldin⁵⁰, D.V. Bandurin⁵⁹, S. Banerjee³⁰, E. Barberis⁶³, A.-F. Barfuss¹⁵, P. Bargassa⁸⁰, P. Baringer⁵⁸, J. Barreto², J.F. Bartlett⁵⁰, U. Bassler¹⁸, D. Bauer⁴⁴, S. Beale⁶, A. Bean⁵⁸, M. Begalli³, M. Begel⁷³, C. Belanger-Champagne⁴², L. Bellantoni⁵⁰, A. Bellavance⁵⁰, J.A. Benitez⁶⁵, S.B. Beri²⁸, G. Bernardi¹⁷, R. Bernhard²³, I. Bertram⁴³, M. Besançon¹⁸, R. Beuselinck⁴⁴, V.A. Bezubov⁴⁰, P.C. Bhat⁵⁰, V. Bhatnagar²⁸, G. Blazey⁵², S. Blessing⁴⁹, K. Bloom⁶⁷, A. Boehnlein⁵⁰, D. Boline⁶², T.A. Bolton⁵⁹, E.E. Boos³⁹, G. Borissov⁴³, T. Bose⁶², A. Brandt⁷⁸, R. Brock⁶⁵, G. Brooijmans⁷⁰, A. Bross⁵⁰, D. Brown¹⁹, X.B. Bu⁷, D. Buchholz⁵³, M. Buehler⁸¹, V. Buescher²², V. Bunichev³⁹, S. Burdin^{43,c}, T.H. Burnett⁸², C.P. Buszello⁴⁴, P. Calfayan²⁶, B. Calpas¹⁵, S. Calvet¹⁶, J. Cammin⁷¹, M.A. Carrasco-Lizarraga³⁴, E. Carrera⁴⁹, W. Carvalho³, B.C.K. Casey⁵⁰, H. Castilla-Valdez³⁴, S. Chakrabarti⁷², D. Chakraborty⁵², K.M. Chan⁵⁵, A. Chandra⁴⁸, E. Cheu⁴⁶, D.K. Cho⁶², S. Choi³³, B. Choudhary²⁹, T. Christoudias⁴⁴, S. Cihangir⁵⁰, D. Claes⁶⁷, J. Clutter⁵⁸, M. Cooke⁵⁰, W.E. Cooper⁵⁰, M. Corcoran⁸⁰, F. Coudere¹⁸, M.-C. Cousinou¹⁵, S. Crépe-Renaudin¹⁴, D. Cutts⁷⁷, M. Ćwiok³¹, A. Das⁴⁶, G. Davies⁴⁴, K. De⁷⁸, S.J. de Jong³⁶, E. De La Cruz-Burelo³⁴, K. DeVaughan⁶⁷, F. Déliot¹⁸, M. Demarteau⁵⁰, R. Demina⁷¹, D. Denisov⁵⁰, S.P. Denisov⁴⁰, S. Desai⁵⁰, H.T. Diehl⁵⁰, M. Diesburg⁵⁰, A. Dominguez⁶⁷, T. Dorland⁸², A. Dubey²⁹, L.V. Dudko³⁹, L. Duflo¹⁶, D. Duggan⁴⁹, A. Duperrin¹⁵, S. Dutt²⁸, A. Dyshkant⁵², M. Eads⁶⁷, D. Edmunds⁶⁵, J. Ellison⁴⁸, V.D. Elvira⁵⁰, Y. Enari⁷⁷, S. Eno⁶¹, M. Escalier¹⁵, H. Evans⁵⁴, A. Evdokimov⁷³, V.N. Evdokimov⁴⁰, G. Facini⁶³, A.V. Ferapontov⁵⁹, T. Ferbel^{61,71}, F. Fiedler²⁵, F. Filthaut³⁶, W. Fisher⁵⁰, H.E. Fisk⁵⁰, M. Fortner⁵², H. Fox⁴³, S. Fu⁵⁰, S. Fuess⁵⁰, T. Gadfort⁷⁰, C.F. Galea³⁶, A. Garcia-Bellido⁷¹, V. Gavrilov³⁸, P. Gay¹³, W. Geist¹⁹, W. Geng^{15,65}, C.E. Gerber⁵¹, Y. Gershtein^{49,b}, D. Gillberg⁶, G. Ginther^{50,71}, B. Gómez⁸, A. Goussiou⁸², P.D. Grannis⁷², S. Greder¹⁹, H. Greenlee⁵⁰, Z.D. Greenwood⁶⁰, E.M. Gregores⁴, G. Grenier²⁰, Ph. Gris¹³, J.-F. Grivaz¹⁶, A. Grohsjean¹⁸, S. Grünendahl⁵⁰, M.W. Grünewald³¹, F. Guo⁷², J. Guo⁷², G. Gutierrez⁵⁰, P. Gutierrez⁷⁵, A. Haas⁷⁰, P. Haefner²⁶, S. Hagopian⁴⁹, J. Haley⁶⁸, I. Hall⁶⁵, R.E. Hall⁴⁷, L. Han⁷, K. Harder⁴⁵, A. Harel⁷¹, J.M. Hauptman⁵⁷, J. Hays⁴⁴, T. Hebbeker²¹, D. Hedin⁵², J.G. Hegeman³⁵, A.P. Heinson⁴⁸, U. Heintz⁶², C. Hensel²⁴, I. Heredia-De La Cruz³⁴, K. Herner⁶⁴, G. Hesketh⁶³, M.D. Hildreth⁵⁵, R. Hirosky⁸¹, T. Hoang⁴⁹, J.D. Hobbs⁷², B. Hoeneisen¹², M. Hohlfield²², S. Hossain⁷⁵, P. Houben³⁵, Y. Hu⁷², Z. Hubacek¹⁰, N. Huske¹⁷, V. Hynek¹⁰, I. Iashvili⁶⁹, R. Illingworth⁵⁰, A.S. Ito⁵⁰, S. Jabeen⁶², M. Jaffré¹⁶, S. Jain⁷⁵, K. Jakobs²³, D. Jamin¹⁵, R. Jesik⁴⁴, K. Johns⁴⁶, C. Johnson⁷⁰, M. Johnson⁵⁰, D. Johnston⁶⁷, A. Jonckheere⁵⁰, P. Jonsson⁴⁴, A. Juste⁵⁰, E. Kajfasz¹⁵, D. Karmanov³⁹, P.A. Kasper⁵⁰, I. Katsanos⁶⁷, V. Kaushik⁷⁸, R. Kehoe⁷⁹, S. Kermiche¹⁵, N. Khalatyan⁵⁰, A. Khanov⁷⁶, A. Kharchilava⁶⁹, Y.N. Kharzhev³⁷, D. Khatidze⁷⁰, T.J. Kim³², M.H. Kirby⁵³, M. Kirsch²¹, B. Klima⁵⁰, J.M. Kohli²⁸, J.-P. Konrath²³, A.V. Kozelov⁴⁰, J. Kraus⁶⁵, T. Kuhl²⁵, A. Kumar⁶⁹, A. Kupco¹¹, T. Kurča²⁰, V.A. Kuzmin³⁹, J. Kvita⁹, F. Lacroix¹³, D. Lam⁵⁵, S. Lammers⁵⁴, G. Landsberg⁷⁷, P. Lebrun²⁰, W.M. Lee⁵⁰, A. Leflat³⁹, J. Lellouch¹⁷, J. Li^{78,†}, L. Li⁴⁸, Q.Z. Li⁵⁰, S.M. Lietti⁵, J.K. Lim³², D. Lincoln⁵⁰, J. Linnemann⁶⁵, V.V. Lipaev⁴⁰, R. Lipton⁵⁰, Y. Liu⁷, Z. Liu⁶, A. Lobodenko⁴¹, M. Lokajicek¹¹, P. Love⁴³, H.J. Lubatti⁸², R. Luna-Garcia^{34,d}, A.L. Lyon⁵⁰, A.K.A. Maciel², D. Mackin⁸⁰, P. Mättig²⁷, R. Magaña-Villalba³⁴, A. Magerkurth⁶⁴, P.K. Mal⁴⁶, H.B. Malbouisson³, S. Malik⁶⁷, V.L. Malyshev³⁷, Y. Maravin⁵⁹, B. Martin¹⁴, R. McCarthy⁷², C.L. McGivern⁵⁸, M.M. Meijer³⁶, A. Melnitchouk⁶⁶, L. Mendoza⁸, D. Menezes⁵², P.G. Mercadante⁵, M. Merkin³⁹, K.W. Merritt⁵⁰, A. Meyer²¹, J. Meyer²⁴, J. Mitrevski⁷⁰, N.K. Mondal³⁰, R.W. Moore⁶, T. Moulik⁵⁸, G.S. Muanza¹⁵, M. Mulhearn⁷⁰, O. Mundal²², L. Mundim³, E. Nagy¹⁵, M. Naimuddin⁵⁰, M. Narain⁷⁷, H.A. Neal⁶⁴, J.P. Negret⁸, P. Neustroev⁴¹, H. Nilsen²³, H. Nogima³, S.F. Novaes⁵, T. Nunnemann²⁶, G. Obrant⁴¹, C. Ochando¹⁶, D. Onoprienko⁵⁹, J. Orduna³⁴, N. Oshima⁵⁰, N. Osman⁴⁴, J. Osta⁵⁵, R. Otec¹⁰, G.J. Otero y Garzón¹, M. Owen⁴⁵, M. Padilla⁴⁸, P. Padley⁸⁰, M. Pangilinan⁷⁷, N. Parashar⁵⁶, S.-J. Park²⁴, S.K. Park³², J. Parsons⁷⁰, R. Partridge⁷⁷, N. Parua⁵⁴, A. Patwa⁷³, G. Pawloski⁸⁰, B. Penning²³, M. Perfilov³⁹, K. Peters⁴⁵, Y. Peters⁴⁵, P. Pétroff¹⁶, R. Piegaia¹, J. Piper⁶⁵, M.-A. Pleier²², P.L.M. Podesta-Lerma^{34,e}, V.M. Podstavkov⁵⁰, Y. Pogorelov⁵⁵, M.-E. Pol², P. Polozov³⁸, A.V. Popov⁴⁰, W.L. Prado da Silva³, S. Protopopescu⁷³, J. Qian⁶⁴, A. Quadt²⁴, B. Quinn⁶⁶, A. Rakitine⁴³,

M.S. Rangel¹⁶, K. Ranjan²⁹, P.N. Ratoff⁴³, P. Renkel⁷⁹, P. Rich⁴⁵, M. Rijssenbeek⁷², I. Ripp-Baudot¹⁹, F. Rizatdinova⁷⁶, S. Robinson⁴⁴, M. Rominsky⁷⁵, C. Royon¹⁸, P. Rubinov⁵⁰, R. Ruchti⁵⁵, G. Safronov³⁸, G. Sajot¹⁴, A. Sánchez-Hernández³⁴, M.P. Sanders²⁶, B. Sanghi⁵⁰, G. Savage⁵⁰, L. Sawyer⁶⁰, T. Scanlon⁴⁴, D. Schaile²⁶, R.D. Schamberger⁷², Y. Scheglov⁴¹, H. Schellman⁵³, T. Schliephake²⁷, S. Schlobohm⁸², C. Schwanenberger⁴⁵, R. Schwienhorst⁶⁵, J. Sekaric⁴⁹, H. Severini⁷⁵, E. Shabalina²⁴, M. Shamim⁵⁹, V. Shary¹⁸, A.A. Shchukin⁴⁰, R.K. Shivpuri²⁹, V. Siccaldi¹⁹, V. Simak¹⁰, V. Sirotenko⁵⁰, P. Skubic⁷⁵, P. Slattey⁷¹, D. Smirnov⁵⁵, G.R. Snow⁶⁷, J. Snow⁷⁴, S. Snyder⁷³, S. Söldner-Rembold⁴⁵, L. Sonnenschein²¹, A. Sopczak⁴³, M. Sosebee⁷⁸, K. Soustruznik⁹, B. Spurlock⁷⁸, J. Stark¹⁴, V. Stolin³⁸, D.A. Stoyanova⁴⁰, J. Strandberg⁶⁴, M.A. Strang⁶⁹, E. Strauss⁷², M. Strauss⁷⁵, R. Ströhmer²⁶, D. Strom⁵³, L. Stutte⁵⁰, S. Sumowidagdo⁴⁹, P. Svoisky³⁶, M. Takahashi⁴⁵, A. Tanasijczuk¹, W. Taylor⁶, B. Tiller²⁶, M. Titov¹⁸, V.V. Tokmenin³⁷, I. Torchiani²³, D. Tsybychev⁷², B. Tuchming¹⁸, C. Tully⁶⁸, P.M. Tuts⁷⁰, R. Unalan⁶⁵, L. Uvarov⁴¹, S. Uvarov⁴¹, S. Uzunyan⁵², P.J. van den Berg³⁵, R. Van Kooten⁵⁴, W.M. van Leeuwen³⁵, N. Varelas⁵¹, E.W. Varnes⁴⁶, I.A. Vasilyev⁴⁰, P. Verdier²⁰, L.S. Vertogradov³⁷, M. Verzocchi⁵⁰, D. Vilanova¹⁸, P. Vint⁴⁴, P. Vokac¹⁰, M. Voutilainen^{67,f}, R. Wagner⁶⁸, H.D. Wahl⁴⁹, M.H.L.S. Wang⁷¹, J. Warchol⁵⁵, G. Watts⁸², M. Wayne⁵⁵, G. Weber²⁵, M. Weber^{50,g}, L. Welty-Rieger⁵⁴, A. Wenger^{23,h}, M. Wetstein⁶¹, A. White⁷⁸, D. Wicke²⁵, M.R.J. Williams⁴³, G.W. Wilson⁵⁸, S.J. Wimpenny⁴⁸, M. Wobisch⁶⁰, D.R. Wood⁶³, T.R. Wyatt⁴⁵, Y. Xie⁷⁷, C. Xu⁶⁴, S. Yacoub⁵³, R. Yamada⁵⁰, W.-C. Yang⁴⁵, T. Yasuda⁵⁰, Y.A. Yatsunenko³⁷, Z. Ye⁵⁰, H. Yin⁷, K. Yip⁷³, H.D. Yoo⁷⁷, S.W. Youn⁵³, J. Yu⁷⁸, C. Zeitnitz²⁷, S. Zelitch⁸¹, T. Zhao⁸², B. Zhou⁶⁴, J. Zhu⁷², M. Zielinski⁷¹, D. Zieminska⁵⁴, L. Zivkovic⁷⁰, V. Zutshi⁵², and E.G. Zverev³⁹

(The DØ Collaboration)

¹Universidad de Buenos Aires, Buenos Aires, Argentina

²LAFEX, Centro Brasileiro de Pesquisas Físicas, Rio de Janeiro, Brazil

³Universidade do Estado do Rio de Janeiro, Rio de Janeiro, Brazil

⁴Universidade Federal do ABC, Santo André, Brazil

⁵Instituto de Física Teórica, Universidade Estadual Paulista, São Paulo, Brazil

⁶University of Alberta, Edmonton, Alberta, Canada; Simon Fraser University, Burnaby, British Columbia, Canada; York University, Toronto, Ontario, Canada and McGill University, Montreal, Quebec, Canada

⁷University of Science and Technology of China, Hefei, People's Republic of China

⁸Universidad de los Andes, Bogotá, Colombia

⁹Center for Particle Physics, Charles University,

Faculty of Mathematics and Physics, Prague, Czech Republic

¹⁰Czech Technical University in Prague, Prague, Czech Republic

¹¹Center for Particle Physics, Institute of Physics, Academy of Sciences of the Czech Republic, Prague, Czech Republic

¹²Universidad San Francisco de Quito, Quito, Ecuador

¹³LPC, Université Blaise Pascal, CNRS/IN2P3, Clermont, France

¹⁴LPSC, Université Joseph Fourier Grenoble 1, CNRS/IN2P3, Institut National Polytechnique de Grenoble, Grenoble, France

¹⁵CPPM, Aix-Marseille Université, CNRS/IN2P3, Marseille, France

¹⁶LAL, Université Paris-Sud, IN2P3/CNRS, Orsay, France

¹⁷LPNHE, IN2P3/CNRS, Universités Paris VI and VII, Paris, France

¹⁸CEA, Irfu, SPP, Saclay, France

¹⁹IPHC, Université de Strasbourg, CNRS/IN2P3, Strasbourg, France

²⁰IPNL, Université Lyon 1, CNRS/IN2P3, Villeurbanne, France and Université de Lyon, Lyon, France

²¹III. Physikalisches Institut A, RWTH Aachen University, Aachen, Germany

²²Physikalisches Institut, Universität Bonn, Bonn, Germany

²³Physikalisches Institut, Universität Freiburg, Freiburg, Germany

²⁴II. Physikalisches Institut, Georg-August-Universität Göttingen, Göttingen, Germany

²⁵Institut für Physik, Universität Mainz, Mainz, Germany

²⁶Ludwig-Maximilians-Universität München, München, Germany

²⁷Fachbereich Physik, University of Wuppertal, Wuppertal, Germany

²⁸Panjab University, Chandigarh, India

²⁹Delhi University, Delhi, India

³⁰Tata Institute of Fundamental Research, Mumbai, India

³¹University College Dublin, Dublin, Ireland

³²Korea Detector Laboratory, Korea University, Seoul, Korea

³³SungKyunKwan University, Suwon, Korea

³⁴CINVESTAV, Mexico City, Mexico

- ³⁵*FOM-Institute NIKHEF and University of Amsterdam/NIKHEF, Amsterdam, The Netherlands*
³⁶*Radboud University Nijmegen/NIKHEF, Nijmegen, The Netherlands*
³⁷*Joint Institute for Nuclear Research, Dubna, Russia*
³⁸*Institute for Theoretical and Experimental Physics, Moscow, Russia*
³⁹*Moscow State University, Moscow, Russia*
⁴⁰*Institute for High Energy Physics, Protvino, Russia*
⁴¹*Petersburg Nuclear Physics Institute, St. Petersburg, Russia*
⁴²*Stockholm University, Stockholm, Sweden, and Uppsala University, Uppsala, Sweden*
⁴³*Lancaster University, Lancaster, United Kingdom*
⁴⁴*Imperial College, London, United Kingdom*
⁴⁵*University of Manchester, Manchester, United Kingdom*
⁴⁶*University of Arizona, Tucson, Arizona 85721, USA*
⁴⁷*California State University, Fresno, California 93740, USA*
⁴⁸*University of California, Riverside, California 92521, USA*
⁴⁹*Florida State University, Tallahassee, Florida 32306, USA*
⁵⁰*Fermi National Accelerator Laboratory, Batavia, Illinois 60510, USA*
⁵¹*University of Illinois at Chicago, Chicago, Illinois 60607, USA*
⁵²*Northern Illinois University, DeKalb, Illinois 60115, USA*
⁵³*Northwestern University, Evanston, Illinois 60208, USA*
⁵⁴*Indiana University, Bloomington, Indiana 47405, USA*
⁵⁵*University of Notre Dame, Notre Dame, Indiana 46556, USA*
⁵⁶*Purdue University Calumet, Hammond, Indiana 46323, USA*
⁵⁷*Iowa State University, Ames, Iowa 50011, USA*
⁵⁸*University of Kansas, Lawrence, Kansas 66045, USA*
⁵⁹*Kansas State University, Manhattan, Kansas 66506, USA*
⁶⁰*Louisiana Tech University, Ruston, Louisiana 71272, USA*
⁶¹*University of Maryland, College Park, Maryland 20742, USA*
⁶²*Boston University, Boston, Massachusetts 02215, USA*
⁶³*Northeastern University, Boston, Massachusetts 02115, USA*
⁶⁴*University of Michigan, Ann Arbor, Michigan 48109, USA*
⁶⁵*Michigan State University, East Lansing, Michigan 48824, USA*
⁶⁶*University of Mississippi, University, Mississippi 38677, USA*
⁶⁷*University of Nebraska, Lincoln, Nebraska 68588, USA*
⁶⁸*Princeton University, Princeton, New Jersey 08544, USA*
⁶⁹*State University of New York, Buffalo, New York 14260, USA*
⁷⁰*Columbia University, New York, New York 10027, USA*
⁷¹*University of Rochester, Rochester, New York 14627, USA*
⁷²*State University of New York, Stony Brook, New York 11794, USA*
⁷³*Brookhaven National Laboratory, Upton, New York 11973, USA*
⁷⁴*Langston University, Langston, Oklahoma 73050, USA*
⁷⁵*University of Oklahoma, Norman, Oklahoma 73019, USA*
⁷⁶*Oklahoma State University, Stillwater, Oklahoma 74078, USA*
⁷⁷*Brown University, Providence, Rhode Island 02912, USA*
⁷⁸*University of Texas, Arlington, Texas 76019, USA*
⁷⁹*Southern Methodist University, Dallas, Texas 75275, USA*
⁸⁰*Rice University, Houston, Texas 77005, USA*
⁸¹*University of Virginia, Charlottesville, Virginia 22901, USA and*
⁸²*University of Washington, Seattle, Washington 98195, USA*
(Dated: Received 29 June 2009; published 5 November 2009)

We present the first measurement of dijet angular distributions in $p\bar{p}$ collisions at $\sqrt{s} = 1.96$ TeV at the Fermilab Tevatron Collider. The measurement is based on a dataset corresponding to an integrated luminosity of 0.7 fb^{-1} collected with the D0 detector. Dijet angular distributions have been measured over a range of dijet masses, from 0.25 TeV to above 1.1 TeV. The data are in good agreement with the predictions of perturbative QCD and are used to constrain new physics models including quark compositeness, large extra dimensions, and TeV^{-1} scale extra dimensions. For all models considered, we set the most stringent direct limits to date.

PACS numbers: 12.60.Rc, 11.25.Wx, 12.38.Qk, 13.87.Ce

At large momentum transfers, dijet production has the largest cross section of all processes at a hadron collider and therefore directly probes the highest energy regime.

It can be used to test the standard model (SM) at previously unexplored small distance scales and to search for signals predicted by new physics models. The angular

distribution of dijets with respect to the hadron beam direction is directly sensitive to the dynamics of the underlying reaction. While in quantum chromodynamics (QCD) this distribution shows small but noticeable deviations from Rutherford scattering, an excess at large angles from the beam axis would be a sign of new physics processes not included in the SM, such as substructure of quarks (“quark compositeness”) [1, 2, 3], or the existence of additional compactified spatial dimensions (“extra dimensions”) [4, 5, 6, 7, 8]. Earlier measurements of dijet angular distributions and related observables in $p\bar{p}$ collisions at $\sqrt{s} = 1.8$ TeV were used to set limits on quark compositeness [9, 10].

In this Letter we present the first measurement of dijet angular distributions in $p\bar{p}$ collisions at a center-of-mass energy of $\sqrt{s} = 1.96$ TeV. The data sample, collected with the D0 detector during 2004–2005 in Run II of the Fermilab Tevatron Collider, corresponds to an integrated luminosity of 0.7 fb^{-1} . In the experiment and in theory calculations, jets are defined by the Run II midpoint cone jet algorithm [11] with a cone radius of $\mathcal{R} = \sqrt{(\Delta y)^2 + (\Delta\phi)^2} = 0.7$ in rapidity y and azimuthal angle ϕ . Rapidity is related to the polar scattering angle θ with respect to the beam axis by $y = 0.5 \ln[(1 + \beta \cos \theta)/(1 - \beta \cos \theta)]$ with $\beta = |\vec{p}|/E$. We measure distributions in the dijet variable $\chi_{\text{dijet}} = \exp(|y_1 - y_2|)$ in ten regions of dijet invariant mass M_{jj} , where y_1 and y_2 are the rapidities of the two jets with highest transverse momentum p_T with respect to the beam axis in an event. For massless $2 \rightarrow 2$ scattering, the variable χ_{dijet} is related to the polar scattering angle θ^* in the partonic center-of-mass frame by $\chi_{\text{dijet}} = (1 + \cos \theta^*)/(1 - \cos \theta^*)$. The choice of this variable is motivated by the fact that Rutherford scattering is independent of χ_{dijet} . The phase space of this analysis is defined by $M_{jj} > 0.25 \text{ TeV}$, $\chi_{\text{dijet}} < 16$, and $y_{\text{boost}} = 0.5 |y_1 + y_2| < 1$. Together, the χ_{dijet} and y_{boost} requirements restrict the jet phase space to $|y_{\text{jet}}| < 2.4$ where jets are well-reconstructed in the D0 detector and the energy calibration is known to high precision. To minimize sensitivity to correlated experimental and theoretical uncertainties, the χ_{dijet} distributions in the different M_{jj} ranges are normalized by their respective integrals. Based on the measurement, we set limits on quark compositeness [1, 2, 3], large spatial extra dimensions according to the model proposed by Arkani-Hamed, Dimopoulos and Dvali (ADD LED) [4, 5], and TeV^{-1} scale extra dimensions (TeV^{-1} ED) [6, 7, 8].

A detailed description of the D0 detector can be found in Ref. [12]. The event selection, jet reconstruction, jet energy and momentum correction in this measurement follow closely those used in our recent measurement of the inclusive jet cross section [13]. The primary tool for jet detection is the finely segmented uranium-liquid argon calorimeter that has almost complete solid angular coverage $1.7^\circ \lesssim \theta \lesssim 178.3^\circ$ [12]. Events are triggered by

the jet with highest p_T , referred to as p_T^{max} . In each M_{jj} region, events are taken from a single trigger which is chosen such that the smallest p_T^{max} in the M_{jj} region is above the threshold that ensures 100% efficiency. The M_{jj} regions utilize triggers with different prescales, resulting in integrated luminosities of 0.10 pb^{-1} ($M_{jj} < 0.4 \text{ TeV}$), 1.54 pb^{-1} ($0.4 < M_{jj} < 0.5 \text{ TeV}$), 17 pb^{-1} ($0.5 < M_{jj} < 0.6 \text{ TeV}$), 73 pb^{-1} ($0.6 < M_{jj} < 0.8 \text{ TeV}$), 0.5 fb^{-1} ($0.8 < M_{jj} < 1.0 \text{ TeV}$), and 0.7 fb^{-1} ($M_{jj} > 1.0 \text{ TeV}$).

The position of the $p\bar{p}$ interaction is reconstructed using a tracking system consisting of silicon microstrip detectors and scintillating fibers, located inside a 2 T solenoidal magnet [12], and is required to be within 50 cm of the detector center along the beam direction. The jet four-momenta are corrected for the response of the calorimeter, the net energy flow through the jet cone, energy from event pile-up and multiple $p\bar{p}$ interactions, and for systematic shifts in $|y|$ due to detector effects [13]. Cosmic ray backgrounds are suppressed by requirements on the missing transverse momentum in an event [13]. Requirements on characteristics of shower shape are used to suppress the remaining background due to electrons, photons, and detector noise that mimic jets. The efficiency for these requirements is above 97.5%, and the fraction of background events is below 0.1% in all M_{jj} regions.

The χ_{dijet} distributions are corrected for instrumental effects using events generated with PYTHIA v6.419 [14] using tune QW [15] and MSTW2008LO parton distribution functions (PDFs) [16]. The generated particle-level events are subjected to a fast simulation of the D0 detector response, based on parametrizations of resolution effects in p_T , the polar and azimuthal angles of jets, jet reconstruction efficiencies, and misidentification of the event vertex. These parametrizations have been determined either from data or from a detailed simulation of the D0 detector using GEANT [17]. The generated events are reweighted according to the M_{jj} distribution in data. To minimize migrations between M_{jj} regions due to resolution effects, we use the simulation to obtain a rescaling function in M_{jj} that optimizes the correlation between the reconstructed and true values. The bin sizes in the χ_{dijet} distributions are chosen to be much larger than the χ_{dijet} resolution. The bin purity after M_{jj} rescaling, defined as the fraction of all reconstructed events that were generated in the same bin, is between 42% and 68%. We then use the simulation to determine χ_{dijet} bin correction factors for the differential cross sections in the different M_{jj} regions. These also include corrections for the energies of unreconstructed muons and neutrinos inside the jets. The total correction factors for the differential cross sections are typically between 0.9 and 1.0, and always in the range 0.7 to 1.1. The corrected differential cross sections within each M_{jj} range are subsequently normalized to their integrals, providing the corrected, final results for $1/\sigma_{\text{dijet}} \cdot d\sigma/d\chi_{\text{dijet}}$ at the “particle level” as defined

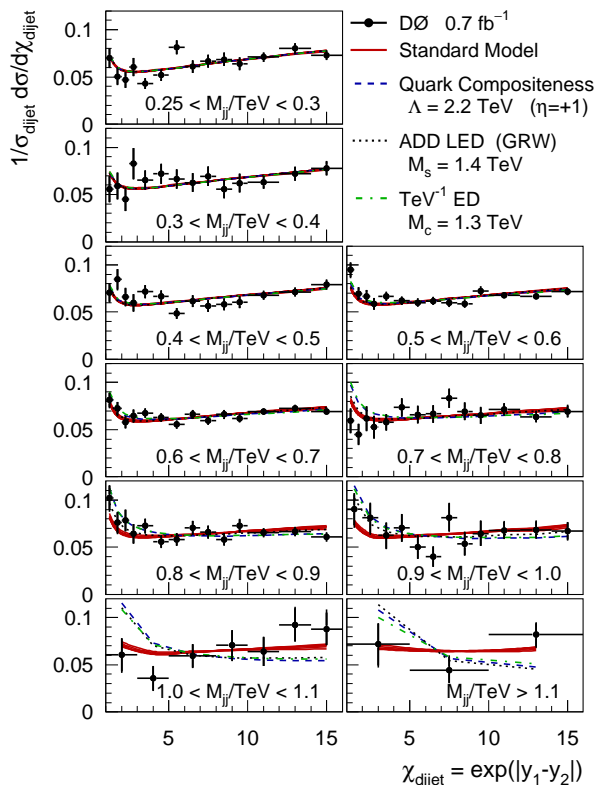


FIG. 1: Normalized differential cross sections in χ_{dijet} compared to standard model predictions and to the predictions of various new physics models. The error bars display the quadratic sum of statistical and systematic uncertainties. The standard model theory band includes uncertainties from scale variations and PDF uncertainties (see text for details).

in Ref. [18].

In order to take into account correlations between systematic uncertainties, the experimental systematic uncertainties are separated into independent sources, for each of which the effects are fully correlated between all data points. In total we have identified 76 independent sources, of which 48 are related to the jet energy calibration and 15 to the jet p_T resolution uncertainty. These are the dominant sources of uncertainty. Smaller contributions are from the jet θ resolution and from the systematic shifts in y . All other sources are negligible. All sources and their effects are documented in Ref. [19]. For $M_{jj} < 1$ TeV ($M_{jj} > 1$ TeV) systematic uncertainties are 1%–5% (3%–11%); they are in all cases less than the statistical uncertainties.

The results are available in Ref. [19] and displayed in Fig. 1. The normalized χ_{dijet} distributions are presented in ten M_{jj} regions, starting from $M_{jj} > 0.25$ TeV, and including one region for $M_{jj} > 1.1$ TeV. The data are compared to predictions from a perturbative QCD calculation at next-to-leading order (NLO) with non-perturbative corrections applied. The non-perturbative corrections are determined using PYTHIA.

They are defined as the product of the corrections due to hadronization and to the underlying event. The NLO results are computed using FASTNLO [20] based on NLOJET++ [21, 22]. All theory calculations use MSTW2008NLO PDFs [16] and the corresponding value of $\alpha_s(M_Z) = 0.120$. The PDF uncertainties are provided by the twenty MSTW2008NLO 90% C.L. eigenvectors. Renormalization and factorization scales μ are varied simultaneously around the central value of $\mu_0 = \langle p_T \rangle$ in the range $0.5 \mu_0 \leq \mu \leq 2 \mu_0$ where $\langle p_T \rangle$ is the average dijet p_T . The quadratic sum of scale and PDF uncertainties is displayed as a band around the central SM value in Fig. 1. The scale (PDF) uncertainties are always below 5% (2%) so the band is nearly a line. The theory, including the perturbative results and the non-perturbative corrections, is in good agreement with the data over the whole M_{jj} range with a χ^2 (defined later) of 127.2 for 120 data points in ten normalized distributions. Based on the agreement of the χ_{dijet} measurement with the SM, we proceed to set limits on quark compositeness, ADD LED, and TeV^{-1} ED models.

Hypothetically, quarks could be made of other particles, as assumed in the quark compositeness model in Ref. [1, 2, 3]. We investigate the model in which all quarks are considered to be composite. The parameters in this model are the energy scale Λ and the sign of the interference term η between the standard model and the new physics terms. The ADD LED model [4, 5] assumes that extra spatial dimensions exist in which gravity is allowed to propagate. Jet cross sections receive additional contributions from virtual exchange of Kaluza-Klein excitations of the graviton. There are two different formalisms (GRW [23] and HLZ [24]). The model parameter is the effective Planck scale, M_S , and the HLZ formalism also includes the subleading dependence on the number n of extra dimensions. The TeV^{-1} ED model [6, 7, 8] assumes that extra dimensions exist at the TeV^{-1} scale. SM production cross sections are modified due to virtual Kaluza-Klein excitations of the SM gauge bosons. In this model, gluons can travel through the extra dimensions, which changes the dijet cross section. The parameter in this model is the compactification scale, M_C .

The new physics contributions have only been calculated to leading order (LO), while the QCD predictions are known to NLO. In this analysis, to obtain the best estimate for new physics processes, we multiply the new physics LO calculations bin-by-bin by the SM k -factors ($k = \sigma_{\text{NLO}}/\sigma_{\text{LO}}$). The k -factors are in the range 1.25–1.5, increasing with M_{jj} and decreasing with χ_{dijet} . Their effects on single bins of the normalized χ_{dijet} distributions within the different M_{jj} regions is below 12%. The new physics cross sections are computed using the matrix elements from Refs. [2, 3, 5, 8]. The theoretical variations (scale variations and PDF uncertainties) are consistently propagated into both the SM and the new physics contributions. Predictions for the different mod-

TABLE I: Expected and observed 95% C.L. limits in units of TeV on various new physics (NP) models for different Bayesian priors, and for the $\Delta\chi^2$ criterion.

Model (parameter)	Prior flat in NP Lagrangian		Prior flat in NP x -section		$\Delta\chi^2 = 3.84$ criterion	
	Expected	Observed	Expected	Observed	Expected	Observed
Quark compositeness (Λ)						
$\eta = +1$	2.91	3.06	2.76	2.84	2.80	2.92
$\eta = -1$	2.97	3.06	2.75	2.82	2.82	2.96
TeV ⁻¹ ED (M_C)	1.73	1.67	1.60	1.55	1.66	1.59
ADD LED (M_S)						
GRW	1.53	1.67	1.47	1.59	1.49	1.66
HLZ $n = 3$	1.81	1.98	1.75	1.89	1.77	1.97
HLZ $n = 4$	1.53	1.67	1.47	1.59	1.49	1.66
HLZ $n = 5$	1.38	1.51	1.33	1.43	1.35	1.50
HLZ $n = 6$	1.28	1.40	1.24	1.34	1.25	1.39
HLZ $n = 7$	1.21	1.33	1.17	1.26	1.19	1.32

els are compared to the χ_{dijet} data and to the SM results in Fig. 1. It is observed that all models predict increased contributions as $\chi_{\text{dijet}} \rightarrow 1$ towards large M_{jj} . The M_{jj} evolution of the excess towards small χ_{dijet} is observed to be different for different models.

We define the χ^2 between data and theory using the Hessian approach [25] which introduces nuisance parameters for all correlated sources of experimental and theoretical uncertainty. The χ^2 is then minimized with respect to all nuisance parameters, and is therefore only a function of the new physics model parameter(s). In most cases χ^2 has the minimum for a new physics mass scale of infinity, corresponding to the SM value. Only for the quark compositeness model with positive interference and for the TeV⁻¹ ED model χ^2 has small minima at $\Lambda = 9.88$ TeV with $\Delta\chi^2 = 0.01$ and $M_C = 2.96$ TeV with $\Delta\chi^2 = 0.28$ below the SM value, respectively.

The χ^2 is then transformed into a likelihood which is used in a Bayesian procedure [10] to obtain 95% C.L. limits on the new physics mass scales Λ , M_C , and M_S in the different models. The prior is chosen to be flat in the new physics mass scale raised to the power in which it appears in the Lagrangian or, alternatively, raised to the power in which it enters the model cross section. While the former has been used in many previous analyses, the latter is statistically preferred for being unbiased in the cross section. Alternatively, we have applied a procedure which defines the 95% C.L. limit as the mass scale at which $\chi^2 - \chi^2_{\text{min}} = 3.84$ [26]. This procedure has the advantage of being independent of an assumed prior. The observed limits and the expectation values are listed in Table I. All observed limits are within one standard deviation of the expected limits.

The limit on M_C obtained in this analysis, while inferior to indirect limits from electroweak precision measurements (Ref. [8] and references therein), is complementary and is the result of the first direct search for TeV⁻¹ extra dimensions at a particle collider. The limits on M_S in the different formalisms of the ADD LED

model are on average slightly higher as compared to recent D0 results from the combination of 1 fb⁻¹ of dielectron and diphoton data in Ref. [27], which were so far the most restrictive limits on ADD LED. Our limits on quark compositeness improve previous results from related dijet observables [9, 10] and are the most stringent limits to date.

In summary, we have presented the first measurement of dijet angular distributions in Run II of the Fermilab Tevatron Collider. This is the first measurement of angular distributions of a hard partonic scattering process at energies above 1 TeV in collider-based high energy physics. The normalized χ_{dijet} distributions are well-described by theory calculations in next-to-leading order in the strong coupling constant and are used to set limits on quark compositeness, ADD large extra dimensions, and TeV⁻¹ extra dimensions models. For the TeV⁻¹ extra dimensions model this is the first direct search at a collider. For all models considered, this analysis sets the most stringent direct limits to date.

We thank the staffs at Fermilab and collaborating institutions, and acknowledge support from the DOE and NSF (USA); CEA and CNRS/IN2P3 (France); FASI, Rosatom and RFBR (Russia); CNPq, FAPERJ, FAPESP and FUNDUNESP (Brazil); DAE and DST (India); Colciencias (Colombia); CONACyT (Mexico); KRF and KOSEF (Korea); CONICET and UBACyT (Argentina); FOM (The Netherlands); STFC and the Royal Society (United Kingdom); MSMT and GACR (Czech Republic); CRC Program, CFI, NSERC and WestGrid Project (Canada); BMBF and DFG (Germany); SFI (Ireland); The Swedish Research Council (Sweden); CAS and CNSF (China); and the Alexander von Humboldt Foundation (Germany).

[a] Visitor from Augustana College, Sioux Falls, SD, USA.

- [b] Visitor from Rutgers University, Piscataway, NJ, USA.
- [c] Visitor from The University of Liverpool, Liverpool, UK.
- [d] Visitor from Centro de Investigacion en Computacion - IPN, Mexico City, Mexico.
- [e] Visitor from ECFM, Universidad Autonoma de Sinaloa, Culiacán, Mexico.
- [f] Visitor from Helsinki Institute of Physics, Helsinki, Finland.
- [g] Visitor from Universität Bern, Bern, Switzerland.
- [h] Visitor from Universität Zürich, Zürich, Switzerland.
- [‡] Deceased.
- [1] E. Eichten, I. Hinchliffe, K. D. Lane, and C. Quigg, *Rev. Mod. Phys.* **56**, 579 (1984); **58**, 1065 (1986).
- [2] P. Chiappetta and M. Perrottet, *Phys. Lett. B* **253**, 489 (1991).
- [3] K. D. Lane, arXiv:hep-ph/9605257.
- [4] N. Arkani-Hamed, S. Dimopoulos, and G. R. Dvali, *Phys. Lett. B* **429**, 263 (1998).
- [5] D. Atwood, S. Bar-Shalom, and A. Soni, *Phys. Rev. D* **62**, 056008 (2000).
- [6] K. R. Dienes, E. Dudas, and T. Gherghetta, *Nucl. Phys. B* **537**, 47 (1999).
- [7] A. Pomarol and M. Quiros, *Phys. Lett. B* **438**, 255 (1998).
- [8] K. Cheung and G. Landsberg, *Phys. Rev. D* **65**, 076003 (2002).
- [9] F. Abe *et al.* (CDF Collaboration), *Phys. Rev. Lett.* **77**, 5336 (1996); **78**, 4307 (1997).
- [10] B. Abbott *et al.* (D0 Collaboration), *Phys. Rev. D* **64**, 032003 (2001).
- [11] G. C. Blazey *et al.*, in *Proceedings of the Workshop: QCD and Weak Boson Physics in Run II*, edited by U. Baur, R.K. Ellis, and D. Zeppenfeld, (Batavia, Illinois, 2000) p. 47, see Section 3.5.
- [12] V. M. Abazov *et al.* (D0 Collaboration), *Nucl. Instrum. Methods Phys. Res. A* **565**, 463 (2006).
- [13] V. M. Abazov *et al.* (D0 Collaboration), *Phys. Rev. Lett.* **101**, 062001 (2008).
- [14] T. Sjöstrand *et al.*, *Comput. Phys. Commun.* **135**, 238 (2001).
- [15] M. G. Albrow *et al.* (TeV4LHC QCD Working Group), arXiv:hep-ph/0610012.
- [16] A. D. Martin, W. J. Stirling, R. S. Thorne and G. Watt, *Eur. Phys. J. C* **63**, 189 (2009).
- [17] R. Brun and F. Carminati, CERN Program Library Long Wwriteup W5013, 1993 (unpublished).
- [18] C. Buttar *et al.*, arXiv:0803.0678, section 9.
- [19] See EPAPS Document No. E-PRLTAO-103-025947 for the measurement results and uncertainty correlations. For more information on EPAPS, see <http://www.aip.org/pubservs/epaps.html>
- [20] T. Kluge, K. Rabbertz, and M. Wobisch, arXiv:hep-ph/0609285.
- [21] Z. Nagy, *Phys. Rev. D* **68**, 094002 (2003).
- [22] Z. Nagy, *Phys. Rev. Lett.* **88**, 122003 (2002).
- [23] G. F. Giudice, R. Rattazzi, and J. D. Wells, *Nucl. Phys. B* **544**, 3 (1999).
- [24] T. Han, J. D. Lykken, and R. J. Zhang, *Phys. Rev. D* **59**, 105006 (1999).
- [25] A. Cooper-Sarkar and C. Gwenlan, in *Proceedings of the Workshop: HERA and the LHC, Part A*, edited by A. De Roeck and H. Jung, (Geneva, Switzerland, 2005), see part 2, section 3.
- [26] C. Amsler *et al.*, *Phys. Lett. B* **667**, 1 (2008).
- [27] V. M. Abazov *et al.* (D0 Collaboration), *Phys. Rev. Lett.* **102**, 051601 (2009).